

# Long-range and high-resolution traffic monitoring based on pulse-compression DAS and advanced vehicle tracking algorithm

Iñigo Corera, Enrique Piñeiro, Javier Navallas, Mikel Sagues and Alayn Loayssa

*Institute of Smart Cities and Department of Electrical, Electronic and Communications Engineering,  
Universidad Pública de Navarra, 31006 Pamplona, Spain  
alayn.loayssa@unavarra.es*

**Abstract:** We demonstrate traffic monitoring over tens of kilometres of road using an enhanced distributed acoustic sensing system based on optical pulse compression and a novel transformed-domain-based processing scheme with enhanced vehicle detection and tracking capabilities. © 2022 The Author(s)

## 1. Introduction

Automatic traffic monitoring schemes have attracted great interest in the past years due to the the growing demand for actionable information for the effective management of transport networks. Distributed acoustic sensors are now starting to be considered in this field, as they provide some unique capabilities, linked to their distributed nature, when compared to other technologies as loop detectors, magnetic sensors, radar sensors, microwave detectors or even video cameras [1, 2].

In this work, we introduce a traffic monitoring scheme deploying, for the first time to our knowledge, optical pulse compression (OPC) implemented in a coherent optical time-domain reflectometry (COTDR) setup [3]. OPC is based on launching into the fiber signals with long duration (high energy) and high time-bandwidth product so that they can be processed upon reception with matched filters to produce high resolution effective pulse widths. This greatly relaxes the trade-off between spatial resolution and range, providing an enhancement in the measurement signal-to-noise ratio (SNR) that is, in principle, proportional to the increased duration (energy) of the pulse [4]. We also introduce a new vehicle detection and tracking algorithm based on a novel transformed domain, in which each point corresponds to a specific straight segment that can be related to vehicle trajectories in the non-transformed domain. The technique has been experimentally tested by performing live measurements along a 40-km telecommunication fiber cable running in a buried microduct pipe along a road opened to traffic.

## 2. Installation of the fiber and sensor configuration

The experiments were performed on a spare dark fiber on a 40-km telecommunication fiber cable which is currently used by Gobierno de Navarra to connect two of its premises. The cable is installed buried in the shoulder of a two-way road inside a microduct pipe using the conventional air blowing method. Vehicles circulating on the road generate small vibrations on the pavement which propagate through the ground, reaching the optical fibers inside the cable. These vibrations are detected by the DAS sensor, so that a signal processing scheme can be implemented to detect and track the vehicle. All the measurements shown in this paper were performed simultaneously over the entire length of the fiber, but the specific data highlighted in the figures correspond to the one-kilometre section of the road that is shown in Fig. 1 (a). This location was selected because a video camera could be used to monitor the whole road section and provide an independent verification for the vehicule detection and tracking provided by our sensor.

Distributed acoustic measurements were carried out using a sensor prototype, implementing the coherent OTDR configuration shown in Fig. 1 (b). In this setup, the output of a narrow linewidth laser source is split into two branches. One branch is directly connected to the local oscillator input of a homodyne receiver that comprises a 90° dual-polarization optical hybrid and four balanced detectors, so that polarization diversity is provided. The other branch is fed to a Mach-Zehnder electrooptic modulator (MZ-EOM) that in the experiments is used to translate to the optical domain the linear frequency modulated (LFM) pulses, that are generated by an arbitrary waveform generator (AWG). The MZ-EOM is biased at minimum transmission so that it generates optical double-sideband suppressed-carrier (ODSB-SC) modulation. LFM pulses with 4- $\mu$ s duration and 50-MHz peak-to-peak frequency deviation centered at 50-MHz are used in these measurements. Therefore, in the optical domain 2 simultaneous LFM pulses (one at each side of the optical carrier) are obtained. The resulting spatial resolution after matched

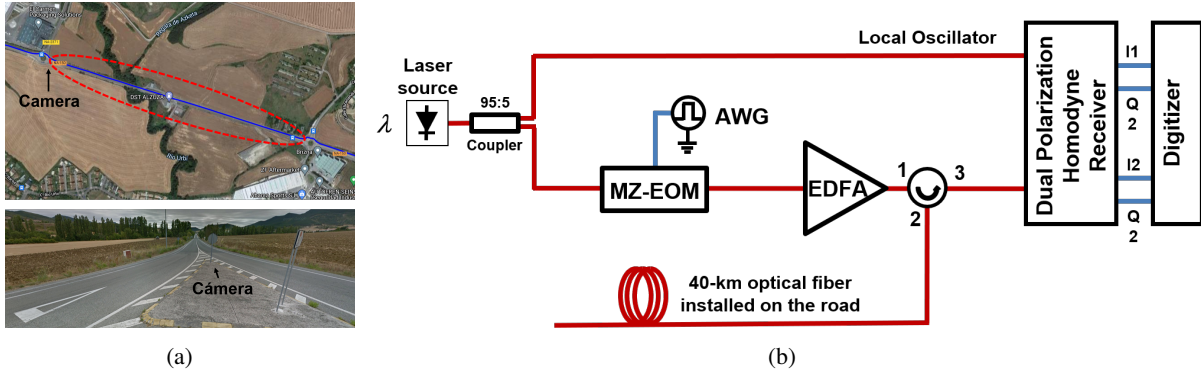


Fig. 1: (a) Section of the telecommunications cable link. (b) Experimental setup.

filtering in reception is 2-m. The output of the MZ-EOM is amplified in an EDFA and launched into the sensing fiber. Finally, the backscattered signal from the fiber is detected in the homodyne receiver and then digitized and post processed in a computer. The pulse repetition frequency was set to 200 Hz, as this was found to be enough to carry out the subsequent signal processing required to detect and track vehicles.

A first preprocessing stage is applied to the raw DAS recording in order to combine the information of the different pulsed sidebands, which experience different Rayleigh scattering statistics, to compensate fading, compensate fading, and remove spurious interferences. This stage is based on the application of the rotated-vector-sum method [5], with a previous spatial moving averaging with a length of 6 m, a summation of the optical field vectors corresponding to the different sidebands, the extraction of the phase from the resultant optical field vector and the computation of the phase difference between samples separated by a gauge length of 6 m so that enough granularity was provided for accurate detection of individual vehicles. Then, the phase data is filtered with a filter with a band pass band from 0.3 to 3.5 Hz, where the fundamental quasi-static components that are dominant in traffic seismic signals are concentrated. After applying this signal preprocessing steps, high sensitivity and resolution signals are obtained, which are then fed to the vehicle detection and tracking algorithm.

### 3. Automatic traffic detection and tracking

Fig. 2 (a) depicts a heat-map displaying the differential phase detected by the DAS sensor along different times (vertical axis) and locations (horizontal axis) corresponding to the 1-km section of the two-way road in Fig. 1 (a). The aim of the system is to provide, from this preprocessed DAS recording, the trajectories of the vehicles passing through the monitored road; i.e., automatically identify the vehicles and provide their spatial position along the road as a function of time. To achieve this goal, the traffic detection and tracking algorithm is divided in two steps: local segment detection and segment tracking.

When considering a short time interval, we can assume that vehicles are moving at a constant velocity, implying a locally linear segment signature in the DAS recording. Therefore, the recording is divided in processing blocks corresponding to short time intervals, so that straight segments corresponding to moving vehicles are to be detected at each of these blocks. Specifically, the processing blocks comprise a time span,  $\Delta t$ , of 5 s. Blocks are calculated every  $\delta t = 0.35$  s, so that the temporal overlapping between consecutive blocks is 4.65 s. Two non-consecutive blocks are marked with black square boxes in Fig. 2 (a) and shown with more detail in Fig. 2 (c).

The segment detection algorithm applied at each block relies on a newly proposed transformed domain, in which each point corresponds to a specific straight segment in the normal non-transformed recording domain. Detecting vehicle segments corresponds to detecting local maxima in this new domain. This transform is an evolution of that proposed in [1], which can be considered as an extension of the Hough Transform that operates with non-binary valued signals.

Let  $F(t_n, d_k) = F[n, k]$  be the differential phase of a certain  $N \times K$  processing block in which segment detection is to be applied, where  $t_n$  represents the time instants within the block time interval, and  $d_k$  the spatial positions along the optical fiber, with  $1 \leq n \leq N$  and  $1 \leq k \leq K$  the corresponding temporal and spatial samples. The first step is to compute the transform  $M(r_i, s_j) = M[i, j]$  of the processing block at each point of the transformed domain. This computation essentially consists of calculating the median of all sample values of the block  $F(t_n, d_k)$  within a certain straight segment defined by the parameters of the transformed domain  $(r_i, s_j)$ , where  $r_i$  is the starting spatial position of the segment at the block starting time; and  $s_j$  is the ending position of the segment at the block ending time. Hence, the segment in the signal domain comprises a set of time-space tuples  $(t_n, d_n)$ , where times

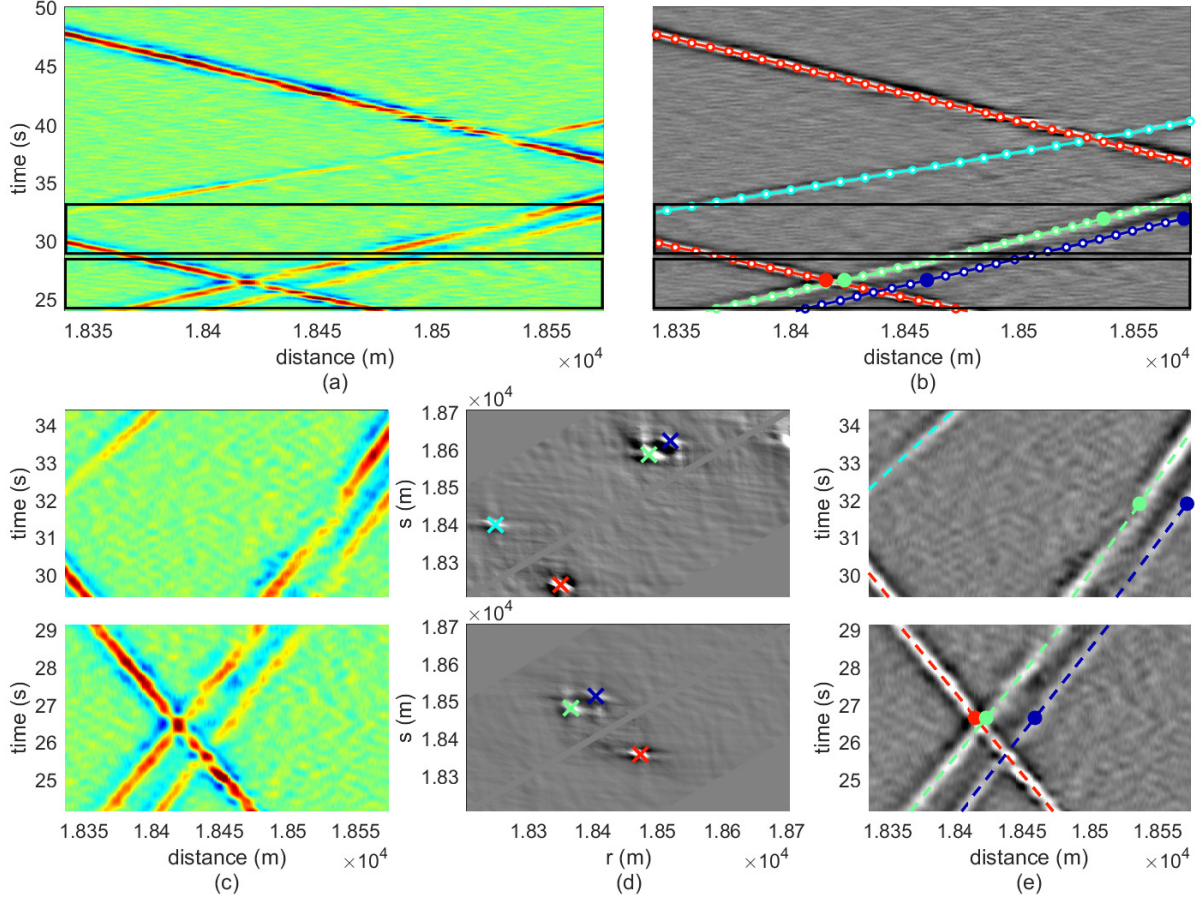


Fig. 2: (a) Measured vibration intensity and (b) results of the vehicle detection and tracking algorithm. (c) Detail of the measured vibration intensity (d) transformed-domain and (e) resulting segments after segmentation, for the two time-distance blocks marked with black square boxes in (a).

are given by the sampling instants  $t_n$  and spatial positions are computed as:

$$d_n = r_i + \frac{s_j - r_i}{\Delta t} t_n \quad (1)$$

In order to work with a discretized spatial domain, a rounding operation must be applied over the segment positions  $d_n$  so that each of them exactly corresponds to a certain sampling position of the signal  $d_k$ . Thus,  $d_n \leftarrow d_k$  such that it minimizes  $|d_n - d_k|$ . The median signal values within the segment, i.e., the transform value at  $(r_i, s_j)$  is given by

$$M(r_i, s_j) = \text{median} \left[ \{F(t_n, d_n)\}_{n=1}^N \right] \quad (2)$$

The sampling resolution of the transformed axes  $r_i$  and  $s_j$  is set to 1.8 m. An additional restriction is imposed to the points of the transformed domain to be computed. Only those points for which the segment represents a moving velocity in the range [2, 60] m/s are computed.

Once the transformed map  $M(r_i, s_j) = M[i, j]$  is obtained, local maxima of the map are extracted. Note that the locations of these maxima correspond to segments of the signal in which the median amplitude value is higher, implying a high probability that these segments correspond to the passage of a moving vehicle. Therefore, after computing a segment detection stage for a certain processing block, a set of local maxima in the transformed domain  $\{(r_l, s_l)\}_{l=1}^L$  is available (marked with colored crosses in Fig. 2 (d)), where  $l$  indexes the different detected and validated locations. These points correspond to specific straight segments in the non-transformed domain considered as potential moving vehicles, as shown in Fig. 2 (e), where the colors of each trajectory correspond to those of the local maxima in Fig. 2 (d).

Once local segments are detected at each processing block, the next step is to join these segments among the different blocks so that arbitrarily large trajectories corresponding to detected moving vehicles are obtained. The input

of the tracking algorithm is the set of local maximum points in the transformed domain  $\{p_l^m\}_{l=1}^{L_m} = \{(r_l^m, s_l^m)\}_{l=1}^{L_m}$  detected at each processing block, where  $m$  indexes the different processing blocks, with  $L_m$  the number of points of the  $m$ th block. The proposed tracking algorithm dynamically initiates, expands and ends trajectories as the sets of points of new blocks are being considered. Trajectories are defined as sequences of points in the transformed domain, where each point belongs to a different processing block. In this way, the  $q$ th trajectory is denoted as  $\{w_q^m\}_{m=m_{\text{ini}q}}^{m_{\text{end}q}} = \{(r_{w_q}^m, s_{w_q}^m)\}_{m=m_{\text{ini}q}}^{m_{\text{end}q}}$ , where  $m_{\text{ini}q}$  and  $m_{\text{end}q}$  are the indexes of the processing blocks in which the trajectory begins and ends; and  $(r_{w_q}^m, s_{w_q}^m)$  is the point location in the transformed domain for the trajectory  $q$  in the block  $m$ .

Each point of the first processing block give rises to the generation of a new trajectory, which is initialized containing only the point under consideration. In an iterative procedure, the points of new processing blocks are joined to the already existing trajectories by means of a distance criterion. This process also enables the generation of new trajectories, as well as the termination of existing ones, which is a key feature in a real-field environment. Next, for each processing block, the distance between the point of each provisional trajectory  $q$  in the  $m$ th processing block (the current endpoint of the trajectory), and each point  $l$  detected in the  $m+1$ th processing block is calculated

$$\text{dist}[w_q^m, p_l^{m+1}] = \sqrt{D_r^2 + D_s^2} \quad (3)$$

where

$$D_r = (r_{w_q}^m - r_l^{m+1}) + \frac{\delta t}{2\Delta t} (s_{w_q}^m - r_{w_q}^m + s_l^{m+1} - r_l^{m+1}) \quad (4)$$

$$D_s = (s_{w_q}^m - s_l^{m+1}) + \frac{\delta t}{2\Delta t} (s_{w_q}^m - r_{w_q}^m + s_l^{m+1} - r_l^{m+1}) \quad (5)$$

Points of block  $m+1$  are joined to the provisional trajectories in an iterative process, in which, at each iteration, the combination  $w_q^m, p_l^{m+1}$  with the lowest distance gives rise to a new union. This process ends when there is no joint whose distance is less than the maximum allowed distance. Once a trajectory is closed, if its length is shorter than a certain number of points, the trajectory is discarded. Otherwise, it is incorporated to the set of definitive trajectories. Finally, a last step is applied to describe these trajectories as a sequence of time-distance tuples in the non-transformed domain. In this domain each trajectory actually represents a sequence of segments among the different processing blocks. Therefore, the time and position in the middle of the segment is chosen as the time-distance coordinate of the trajectory within the segment. Fig. 2 (b) represents these trajectories, as colored points superimposed to the grey-scale map of the signal in Fig. 2 (a), showing excellent result.

#### 4. Discussion and conclusions

We have demonstrated a long-range and high-resolution automatic traffic monitoring scheme which takes advantage of the enhanced sensing capabilities provided by optical pulse compression in distributed phase-sensitive optical time-domain reflectometry. In addition, a vehicle detection and tracking algorithm has been developed, based on a novel transformed domain, enabling high-accuracy non-machine-learning-based traffic monitoring, which could be an advantage in certain scenarios as it does not require a training stage. Further work should focus on exploring the capabilities of the vehicle detection algorithm to provide vehicle classification or other valuable information for traffic management.

**Funding.** This work was supported in part by European Union “Next generationEU”/PRTR and MCIN/AEI/10.13039/501100011033 under grant PDC2021-121172-C21, in part by FEDER “A way to make Europe” and MCIN/AEI/10.13039/501100011033 under grant PID2019-107270RB, and in part by Gobierno de Navarra under grant PC210-211 FIBRATRAFIK. The authors would like to thank Gobierno de Navarra and NASERTIC S.A.U for their support by giving access to the dark fiber deployed in this work.

#### References

1. K. Chambers, “Using das to investigate traffic patterns at brady hot springs, nevada, usa,” *The Lead*. Edge p. 819–827 (2020).
2. E. Catalano, A. Coscetta, E. Cerri, N. Cennamo, L. Zeni, and A. Minardo, “Automatic traffic monitoring by  $\phi$ -otdr data and hough transform in a real-field environment,” *Appl. Opt.* **60**, 3579–3584 (2021).
3. O. H. Waagaard, E. Rønnekleiv, A. Haukanes, F. Stabo-Eeg, D. Thingbø, S. Forbord, S. E. Aasen, and J. K. Brenne, “Real-time low noise distributed acoustic sensing in 171 km low loss fiber,” *OSA Continuum* **4**, 688–701 (2021).
4. A. Loayssa, M. Sagues, and A. Eyal, “Phase noise effects on phase-sensitive otdr sensors using optical pulse compression,” *J. Light. Technol.* pp. 1–1 (2021).
5. D. Chen, Q. Liu, and Z. He, “Phase-detection distributed fiber-optic vibration sensor without fading-noise based on time-gated digital ofdr,” *Opt. Express* **25**, 8315–8325 (2017).